



**HAL**  
open science

## Sliding mode reference conditioning for path following applied to an AUV

Juan Luis Rosendo, Benoit Clement, Fabricio Garelli

► **To cite this version:**

Juan Luis Rosendo, Benoit Clement, Fabricio Garelli. Sliding mode reference conditioning for path following applied to an AUV. 10th IFAC Conference on Control Applications in Marine Systems (CAMS 2016), Sep 2016, Trondheim, Norway. hal-01368470

**HAL Id: hal-01368470**

**<https://ensta-bretagne.hal.science/hal-01368470>**

Submitted on 6 Nov 2017

**HAL** is a multi-disciplinary open access archive for the deposit and dissemination of scientific research documents, whether they are published or not. The documents may come from teaching and research institutions in France or abroad, or from public or private research centers.

L'archive ouverte pluridisciplinaire **HAL**, est destinée au dépôt et à la diffusion de documents scientifiques de niveau recherche, publiés ou non, émanant des établissements d'enseignement et de recherche français ou étrangers, des laboratoires publics ou privés.

# Sliding mode reference conditioning for path following applied to an AUV. <sup>★</sup>

Juan Luis Rosendo <sup>\*</sup> Benoit Clement <sup>\*\*</sup> Fabricio Garelli <sup>\*\*\*</sup>

<sup>\*</sup> CONICET and Universidad Nacional de La Plata, C.C.91 (1900), La Plata, Argentina (e-mail: juanluisrosendo@gmail.com)

<sup>\*\*</sup> Lab-STICC, UMR CNRS 6585, ENSTA Bretagne, 29806 Cedex 9, France (e-mail: benoit.clement@ensta-bretagne.fr)

<sup>\*\*\*</sup> CONICET and Universidad Nacional de La Plata, C.C.91 (1900), La Plata, Argentina (e-mail: fabricio@ing.unlp.edu.ar)

**Abstract:** This work presents a dynamic model for an autonomous underwater vehicle (AUV), a validation of this model together with the simulator obtained from its application and an implementation of sliding mode reference conditioning (SMRC). This last technique is proposed in order to follow a path at maximum speed with bounded errors in a dynamical framework, taking care of the saturation in systems actuators, resulting in an improvement of the path tracking time.

*Keywords:* Sliding mode, Robotics, Simulators, AUV, Path following, Actuator constraints.

## 1. INTRODUCTION

Path tracking is a normal duty in robotics, from industrial applications to mobile robots. The objective is to follow a path with accuracy and as fast as possible, between these contradictory purposes arises the main issues of control tuning. Several problems emerge from this, for instance if a path with tight curves is considered or if a short time is desired to complete the path, it will generate actuator saturations. In these applications, we can remark that the path to follow is given as vector input that can be parametrized in terms of a motion parameter. This idea of such a parametrization has been applied in Nenchev (1995), Nechev and Uchiyama (1997), and Garelli et al. (2010) for manipulators.

In this kind of applications system constraints and bounded desired error define the maximum speed of path tracking. Considering traditional controls, three approaches can be derived:

- (1) To use a fixed tracking speed, that never saturates the robot actuators.
- (2) To use a fixed tracking speed but higher than the previous one, it means that at least it saturates the actuators in some point of the path followed.
- (3) To use a variable tracking speed, calculated for each point of the path taking in consideration the constraints of the system.

It is clear that the first two options are not optimal: (1) does not exploit the maximum of the actuators, and (2) results in an unnecessary error in the track following. On the other hand, the (3) option looks more promising but in general the online calculation for each point is not simple.

<sup>★</sup> This research is partially supported by Eiffel scholarship from France Government, by CONICET (PIP0361 and 0237), MIN-CYT(PICT2394) and UNLP(I164), Argentina.

In this paper, a simple way to implement the approach (3) is experimentally tested. This idea was presented in Garelli et al. (2010) for a cinematic model, and we expand this to a dynamic model. For the demonstration, the methodology is applied to the AUV Ciscrea, showed in fig. 6 as their specifications details in Table 1. This kind of robot is usually designed to operate in the ocean environment, for this, their hydrodynamic model naturally suffers from numerous uncertainties. Due to these identification and modeling problems, this is an interesting plant to model an test the proposed technique.

This works is organized in the following way, section 2 proposes an AUV model for control, then section 3 gives the details for the control technique, section 4 is dedicated to experimental results, and finally in section 5 some conclusions are given.

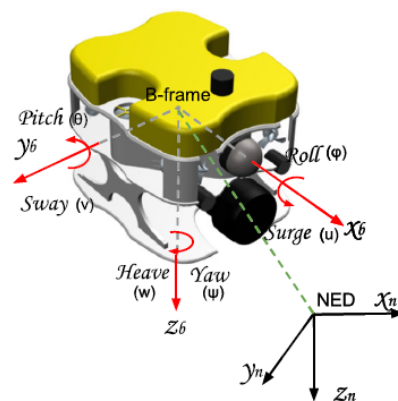


Fig. 1. B-frame and NED-frame of Underwater Vehicles

Size	0.525m (L) 0.406m (W) 0.395m (H)
Weight in air	15.56kg (without payload and floats)
Controllable directions	Surge, Sway, Heave and Yaw
Propulsion	2 vertical and 4 horizontal propellers
Speed	2 knots (Surge) and 1 knot (Sway, Heave)
Depth Rating	50m
On-board Battery	2-4 hours

Table 1. Ciscrea characteristics

## 2. AUV MODELING

### 2.1 Modeling

The mathematical description of underwater vehicle dynamics is essential for an robust control design. Modeling of underwater vehicles involves two parts of study: kinematics and dynamics. In this work is used the modeling ideas of Fossen (2002) and numerical values obtained in Yang et al. (2015). Based on Fossen (2002) and SNAME (1950) two coordinate systems are introduced: a NED-frame (North East Down) and a B-frame (Body fixed reference) for the localization as can be see in figure 1. In this model all distances will be in meters, angles in radians and positive clockwise. The position vector  $\eta$ , velocity vector  $\nu$  and force vector  $\tau$  are defined as:

$$\begin{aligned} \eta &= [x, y, z, \phi, \theta, \psi]^T \\ \nu &= [u, v, w, p, q, r]^T \\ \tau &= [X, Y, Z, K, M, N]^T \end{aligned} \quad (1)$$

According to Fossen (2002), rigid-body hydrodynamic forces and moments can be linearly superimposed. Furthermore, the overall non-linear underwater model is characterized by two parts, the rigid-body dynamic (eq. 2) and hydrodynamic formulations (eq. 3) (hydrostatics included). Parameter definitions are given in Table 2.

$$M_{RB}\dot{\nu} + C_{RB}(\nu)\nu = \tau_{env} + \tau_{hydro} + \tau_{pro} \quad (2)$$

$$\tau_{hydro} = -M_A\dot{\nu} - C_A(\nu)\nu - D(|\nu|)\nu - g(\eta) \quad (3)$$

Parameter	Description
$M_{RB}$	AUV rigid-body mass and inertia matrix
$M_A$	Added mass matrix
$C_{RB}$	Rigid-body induced coriolis-centripetal matrix
$C_A$	Added mass induced coriolis-centripetal matrix
$D( \nu )$	Damping matrix
$g(\eta)$	Restoring forces and moments vector
$\tau_{env}$	Environmental disturbances(wind,waves and currents)
$\tau_{hydro}$	Vector of hydrodynamic forces and moments
$\tau_{pro}$	Propeller forces and moments vector

Table 2. Nomenclature of AUV Model

In the present application  $M_{RB}$  is obtained from Yang et al. (2015), in addition as the vehicle speed is low  $C_{RB}$  and  $C_A$  are neglected,  $C(\nu) \approx 0$ . The restoring forces and moments vector  $g(\eta)$  is composed of the forces and torque produced by the weight and the buoyancy forces. It can be expressed as in eq. 4 where  $BG = [BG_x, BG_y, BG_z]^T$  is the distance from the center of gravity (CG) to the buoyancy center (CB),  $\rho$  is the fluid density,  $vol$  is the displaced fluid volume,  $g$  is the gravity acceleration and  $m$  is the AUV mass.

$$g(\eta) = \begin{bmatrix} -(m - \rho vol)g \sin \theta \\ (m - \rho vol)g \cos \theta \sin \phi \\ (m - \rho vol)g \cos \theta \cos \phi \\ -BG_y mg \cos \theta \cos \phi + BG_z mg \cos \theta \sin \phi \\ -BG_z mg \sin \theta + BG_x mg \cos \theta \sin \phi \\ -BG_x mg \cos \theta \sin \phi - BG_y mg \sin \theta \end{bmatrix} \quad (4)$$

For Ciscrea robot, CB and CG are really close so it is possible to consider them in the same place and in the geometrical center of the robot.

The marine disturbances, such as wind, waves and current contribute to  $\tau_{env}$ . But for an underwater vehicle, only current is considered since wind and waves have negligible effects on AUV during underwater operations.

In order to transform the model in B-frame to a NED-frame, a transformation  $J(\Theta)$  is made in eq. 5, according to eq. 2 and 3. This transformation matrix can be consulted in Yang et al. (2015).

$$M^*\dot{\eta} + D^*(|\nu|)(\dot{\eta}) + g^*(\eta) = \tau_{pro} + \tau_{env} \quad (5)$$

with:

$$\begin{aligned} M^* &= J^{-T}(\Theta)(M_{RB} + M_A)J^{-1}(\Theta), \\ D^*(|\nu|) &= J^{-T}D(|\nu|)J^{-1}(\Theta), \\ g^*(\eta) &= J^{-T}g(\eta), \quad \Theta = [\phi, \theta, \psi]^T. \end{aligned}$$

From this transformation two hydrodynamic parameters have to be precised:

- $M_A \in \mathfrak{R}^{6 \times 6}$ : added mass, is a virtual concept representing the hydrodynamic forces and moments. Any accelerating emerged-object would encounter this  $M_A$  due to the inertia of the fluid.
- $D(|\nu|) \in \mathfrak{R}^{6 \times 6}$ : damping in the fluid, this parameter consists of four additive parts: Potential damping, wave drift damping, skin friction, and vortex shedding damping. The first two could be dismissed in this application, and the others could be approximated by a linear and a quadratic matrices,  $D_L$  and  $D_N$  respectively, as is shown in eq. 6 (Yang et al. (2015), Fossen (2002)).

$$D(|\nu|) = D_L + D_N|\nu| \quad (6)$$

The final model used in the simulator can be represented by eq. 7, where torque of propellers are affected by a transformation from each propeller frame to the B-frame, and extra cross relations between equations due to the angular momentum are considered. Moreover some additional notations have to be introduced:

- $T_i$  is the  $i$ -thruster of the robot for which  $\phi_{t_i}$ ,  $\theta_{t_i}$ ,  $\psi_{t_i}$  denote respectively the roll, pitch and heading of it in B-frame expressed with respect to B-frame.
- $D_{Ni}$  is the non linear damping coefficient for  $i$ -direction.
- $D_{Li}$  is the linear damping coefficient for  $i$ -direction.

### 2.2 Simulator and model validation

The proposed model is used for the implementation of a simulator in the Matlab Simulink software, the numerical values of the model related to the hydrodynamic effects were recuperated from the work Yang et al. (2015) and the mechanical values were taken from measures realized over the robot and data provided by the manufacturer.

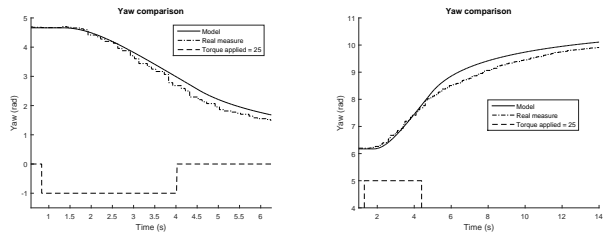
$$\left\{ M_A + \begin{pmatrix} m & 0 & 0 & 0 & 0 & 0 \\ 0 & m & 0 & 0 & 0 & 0 \\ 0 & 0 & m & 0 & 0 & 0 \\ 0 & 0 & 0 & I_x & 0 & 0 \\ 0 & 0 & 0 & 0 & I_y & 0 \\ 0 & 0 & 0 & 0 & 0 & I_k \end{pmatrix} \right\} \begin{pmatrix} \dot{u} \\ \dot{v} \\ \dot{w} \\ \dot{p} \\ \dot{q} \\ \dot{r} \end{pmatrix} = \begin{pmatrix} \sum_{i=1}^n [T_i \cos(\psi_{t_i}) \cos(\theta_{t_i})] - (m - \rho v_{ol})g \sin(\theta) - D_{N_u}|u|u + D_{L_u}u + m(rv - qw) \\ \sum_{i=1}^n [T_i \sin(\psi_{t_i}) \cos(\theta_{t_i})] + (m - \rho v_{ol})g \cos(\theta) \sin(\phi) + D_{N_v}|v|v + D_{L_v}v + m(pw - ru) \\ - \sum_{i=1}^n [T_i \sin(\theta_{t_i})] + (m - \rho v_{ol})g \cos(\theta) \cos(\phi) - D_{N_w}|w|w + D_{L_w}w + m(qu - pv) \\ - \sum_{i=1}^n [T_i (y_{t_i} \sin(\theta_{t_i}) + z_{t_i} \sin(\psi_{t_i}) \cos(\theta_{t_i}))] - D_{N_p}|p|p + D_{L_p}p + (I_y - I_z)qr \\ \sum_{i=1}^n [T_i (z_{t_i} \cos(\psi_{t_i}) \cos(\theta_{t_i}) + x_{t_i} \sin(\theta_{t_i}))] - D_{N_q}|q|q + D_{L_q}q + (I_z - I_x)rp \\ \sum_{i=1}^n [T_i (x_{t_i} \sin(\psi_{t_i}) \cos(\theta_{t_i}) - y_{t_i} \cos(\psi_{t_i}) \cos(\theta_{t_i}))] - D_{N_r}|r|r + D_{L_r}r + (I_x - I_y)pq \end{pmatrix} \quad (7)$$

Two additional effects were considered in the simulator:

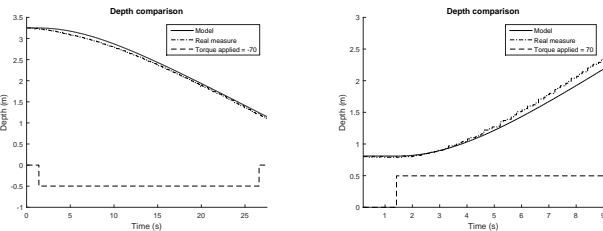
- An additional delay that is present in the depth sensor which was estimated in 0.5 s.
- The non linear conversion between the digital torque (-127 to 127) signals of command to the real torque in the motors (-6 Nm to 6 Nm). This conversion was estimated from measures realized over the robot.

The model validation is performed by time responses comparisons between the simulations and pool tests. In this paper we limit this comparison to open loop turn, emerge and sink maneuvers (fig. 2). The main characteristics are validated at low frequency. This means that any control system have to include a roll off effect if validated on simulations.

In this section, an useful simulation tool has been presented. It has been validated by test in the ENSTA Bretagne pool and it is used for intensive simulations for control laws validation. Moreover the proposed simulator is used for educational purposes for marine robotics.



(a) Turning maneuvering to left T=25 (b) Turning maneuvering to right T=25



(c) Emerge maneuvering T=70 (d) Sink maneuvering T=70

Fig. 2. Open loop validation.

### 3. SLIDING-MODE CONDITIONING ALGORITHM

In this section the basic ideas of sliding modes (SM) technique together with the sliding mode reference condition

(SMRC) are reviewed in order to apply them to the path following of an AUV.

#### 3.1 Background

The sliding modes are originally developed for dynamic systems whose essential open-loop behavior can be modeled adequately with ordinary differential equations. In this systems when we apply a discontinuous control action, usually referred as variable structure control (VSC), it is obtained a feedback system, called variable structure system (VSS), which is governed by ordinary differential equations with an associated switching function that determines a manifold on the state space (sliding surface). According to the sign of the switching function, the control signal takes different possible values, leading to a discontinuous control law. The idea is to enforce the state to reach the prescribed sliding surface and then to slide on it through a very fast switching action. Once this particular mode of operation is established, known as sliding mode (SM), the prescribed manifold imposes the new system dynamics.

The design procedure consists of two stages. First, the equation of the manifold where the system slides is selected in accordance with some performance criterion for the desired dynamics. Then, the discontinuous control should be found such that the systems states reach the manifold and sliding mode exists on this manifold. In order to present the theory, let us consider the dynamical system:

$$\begin{cases} \dot{\mathbf{x}} = f(\mathbf{x}) + g(\mathbf{x})u \\ \mathbf{y} = h(\mathbf{x}) \end{cases} \quad (8)$$

Where  $\mathbf{x} \in \mathbb{R}^n$  is the system state,  $u$  is the control signal,  $y$  is the output system, and  $f(\mathbf{x})$ ,  $g(\mathbf{x})$ ,  $h(\mathbf{x})$  are vector fields in  $\mathbb{R}^n$ . The variable structure control law is defined as:

$$u = \begin{cases} u^- & \text{if } \sigma(\mathbf{x}) < 0 \\ u^+ & \text{if } \sigma(\mathbf{x}) > 0 \end{cases} \quad (9)$$

According to the sign of the auxiliary output  $\sigma(\mathbf{x})$ . The sliding surface  $S$  is defined as the manifold where the auxiliary output, also called switching function, vanishes:

$$S = \{\mathbf{x} \in \mathbb{R}^n \mid \sigma(\mathbf{x}) = 0\} \quad (10)$$

If as a result of the switching policy in eq. 9, the reaching condition (eq. 11) locally holds at both sides of the surface, a switching sequence at very high frequency (ideally infinite) occurs, constraining the system state trajectory to slide on S.

$$\begin{cases} \dot{\sigma}(\mathbf{x}) < \mathbf{0} & \text{if } \sigma(\mathbf{x}) > \mathbf{0} \\ \dot{\sigma}(\mathbf{x}) > \mathbf{0} & \text{if } \sigma(\mathbf{x}) < \mathbf{0} \end{cases} \quad (11)$$

For sliding motion to exist on  $S$  (ie. satisfy condition 11), the auxiliary output  $\sigma(\mathbf{x})$  must have unitary relative degree with respect to the discontinuous signal, i.e. its first derivative must explicitly depend on  $u$  (Utkin et al. (2009)).

### 3.2 Sliding mode reference conditioning (SMRC)

In SMRC, an auxiliary loop allows the system to remain in a pre-specified area, when a restriction in the system is going to be violated. Fig. 3 shows how it works.

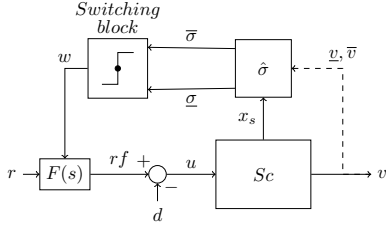


Fig. 3. Block diagram of SMRC technique

This technique has been developed to be applied in VSS, and takes advantage from their non linearities and constraints. The advantages of SMRC are that: (i) it only depends on the relative degree of the model, (ii) it is robust against disturbances and uncertainties, (iii) it is confined to low-power side which facilitates its implementation (see Garelli et al. (2011) and Garelli et al. (2010) for details).

Considering the dynamic system of eq. 8, we are interested in the behavior of a variable  $v$ , restricted to some constraints, in which we are going to apply the SMRC. Let us consider an alternative representation taking  $v$  as a constrained output of the system (8) as in eq. 12. The system described by eq. 12 is represented by the block  $Sc$  in fig. 3.

$$\begin{cases} \dot{\mathbf{x}}_s = f(\mathbf{x}_s) + g(\mathbf{x}_s)u \\ v = h_v(\mathbf{x}_s) \end{cases} \quad (12)$$

$v$  is the bounded variable that has to fulfill user-specified system constraints. To specify the bounds on  $v$ , the following set is defined:

$$\Phi(\mathbf{x}_s) = \{\mathbf{x}_s \mid \phi(v) \leq 0\} \quad (13)$$

Note:  $Sc$  is generically a constrained subsystem of the whole control system, and therefore the variable  $v$  may correspond to any system variable subjected to constraints.

The objective is to find a control input  $u$  which makes the system remaining in the region  $\Phi$ . It means making the  $\Phi$  region invariant. For this the right side of the first eq. 12 must point to the interior of  $\Phi$  at all points on the border surface:

$$\partial\Phi = \{\mathbf{x}_s \mid \mathbf{x}_s \wedge \phi(v) = 0\} \quad (14)$$

This can be guaranteed by the switching policy for the system eq. 12 given by eq. 15 (Garelli et al. (2010)).

$$u = \begin{cases} \leq u^\phi : \mathbf{x}_s \in \partial\Phi \wedge L_g\phi > 0 \\ \geq u^\phi : \mathbf{x}_s \in \partial\Phi \wedge L_g\phi < 0 \\ / \exists : \mathbf{x}_s \in \partial\Phi \wedge L_g\phi = 0 \\ free : \mathbf{x}_s \in \Phi \setminus \partial\Phi \end{cases} \quad (15)$$

with:

- $L_f h(x) : \mathfrak{R}^n \rightarrow \mathfrak{R}$  is the directional derivative or Lie derivative, which denotes the derivative of a scalar field  $h(x) : \mathfrak{R}^n \rightarrow \mathfrak{R}$  in the direction of a vector field  $f(x) : \mathfrak{R}^n \rightarrow \mathfrak{R}^n$

$$L_f h(x) = \frac{\partial h}{\partial x} f(x) \quad (16)$$

- Thus:

$$u^\phi = -L_f\phi/L_g\phi \quad (17)$$

- and where  $L_f\phi > 0$  was assumed without loss of generality.

From eq. 15 results that  $u$  could be free inside the region  $\Phi$ . Usually two approaches are possible:

- $u = 0$ : leaving the system evolve in autonomous way, and the control action becomes active only when the critical constraint is reached.
- $u \neq 0$ : forcing the system to reach the limits of the region and working over the limit surfaces.

Using a trivial case of bounds given by eq. 18, with  $\tilde{v}$  representing the constraints over  $v$ , we can graphically interpret the switching law in fig. 4, where  $w$  is the discontinuous signal generated by the SMRC loop.

$$\sigma(v) = v - \tilde{v} \quad (18)$$

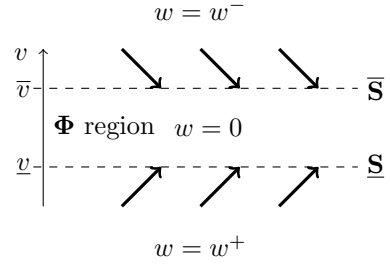


Fig. 4. Graphical interpretation of switching law

To achieve the transient SM on  $\sigma(v) = 0$ , it is necessary to implement an auxiliary loop with a switching function, product of the boundary conditions, that results in a discontinuous signal  $w$ , see fig. 3. In order to smooth the command signal a first order filter is used.

$$F(s) : \begin{cases} \dot{x}_f = \lambda_f x_f + w + r \\ r_f = -\lambda_f x_f \end{cases} \quad (19)$$

Where  $r$  is the original reference of the system and  $\lambda_f \in \mathfrak{R}$  the eigenvalue of the filter.  $\lambda_f$  must to be chosen so that the bandwidth of the filter is higher than the constrained system, in the way the system response is not deteriorated when  $v$  is within its allowed range.

Additionally we could mention that if the system has not relative degree one, nevertheless the SMRC could be applied taking extra system states  $x_s$  in the switching function  $\phi$ , in order to fulfill the condition that its first derivate explicitly depends on the discontinuous action  $w$ . This last is represented in figure 3 with the input of states  $\mathbf{x}_s$  in the boundary condition block  $\hat{\sigma}$ .

This section has revised the background in SMRC, allowing us to show in the next section how to apply it to obtain a path following system that auto-regulates the speed reference.

## 4. EXPERIMENTAL APPLICATION TO DYNAMIC AUV CONTROL

### 4.1 SMRC in AUV

In the previous section a general recall on the SM and SMRC has been made, the SMRC technique is then adapted to the Ciscrea robot in order to generate a variable speed tracking reference compatible with actuator limits.

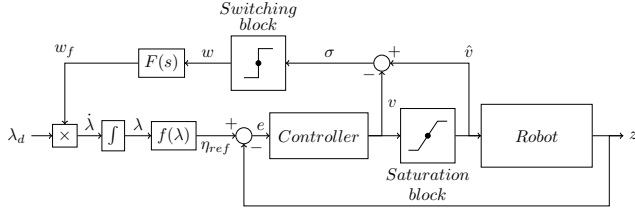


Fig. 5. SMRC proposed for path following

Fig. 5 shows the SMRC technique applied to a simplified model of eq. 7 (only heave direction is considered). Comparing to the notation of subsection 3.2,  $S_c$  is composed by the closed loop formed by the controller, the saturation over the control variable, and the robot system. In addition, we also have the low pass filter  $F(s)$ , and the parametrization of the path,  $f(\lambda)$ . An important consideration is that we suppose that the path is parameterized in terms of a motion parameter and its first derivative has to be continuous. It can be expressed as follows:

$$\eta_{ref} = f(\lambda) \quad \dot{\eta}_{ref} = \frac{\partial f}{\partial \lambda} \dot{\lambda} \quad (20)$$

In this case:

- saturation constraints are imposed on the torque.
- the  $\sigma$  signal, defined as in eq. 18, has relative degree one with respect to the discontinuous signal  $w$ , and a direct saturation is implemented.
- the switching law is defined as:

$$w = \begin{cases} 1 & \text{if } \sigma = 0 \\ 0 & \text{if } \sigma \neq 0 \end{cases} \quad (21)$$

When there is no saturation the switching law makes the discontinuous signal  $w$  take the value 1. After passing the filter a smooth version of  $w$  is multiplied by  $\lambda_d$ , and subsequently integrated to generate a growing parameter  $\lambda$ . This parameter feeds the reference block  $f(\lambda)$  producing the path reference for the controller.

In few words, while there is no saturation the auxiliary loop of SMRC rests inactive and the reference speed is fixed by  $\lambda_d$ . When saturation occurs the signal  $w$  switches between their possible values in order to force a decrease in the speed of the reference (establishing an SM) so the controller could reduce the error position, finally when this condition is over the SMRC loop comes back to the inactive condition.

This configuration has several items that could be adjusted taking into consideration:

- $\lambda_d$ : this parameter has to be chosen large enough to force the saturation of actuators once in the path to be followed, but at the same time not so large that the SMRC loop forces the stop of the reference continuously.

- $F(s)$ : the bandwidth of the first order filter should be selected high enough to allow a fast stop of the system but low to smooth the discontinuous signal  $w$ , in order to not produce chattering effect on the path reference, for a complete analysis of this problem see Garelli et al., 2011.
- Main controller: it has to be able to saturate the controlled variable.

The tuning of these parameters was performed by simulation tests. The values used are:  $\lambda_d = 0.2$ , the cutoff frequency of the low pass filter is  $f_c = 0.2387$  Hz, and the controller is a proportional plus a filtered derivative action (PD) ( $K_p = 541.43, K_d = 250, f_f = 2.3$  Hz). For reasons of space, the simulation results are not included in this work, only the experimental results are shown in the following subsection.

### 4.2 Experiments

The objective is to compare the behavior of a traditional PD control, applied to the Ciscrea heave direction, considering a fixed speed for the path reference against the variable speed technique explained in subsection 4.1. The experiments were conducted in the ENSTA Bretagne pool with a setup conformed for the Ciscrea robot connected to an external computer, to recover the experimental data, see Fig. 6. The classical controller was tuned in order

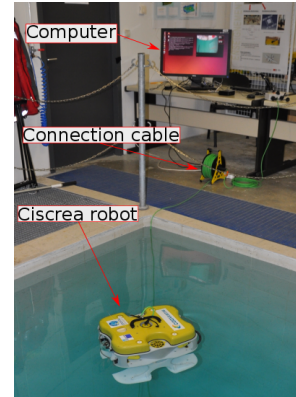


Fig. 6. Ciscrea setup

that the proposed path is on the border of saturating the actuators. On the other hand, the SMRC technique was tuned to have the same bounded position error, see fig. 8, as the classic PD controller.

Fig. 7 shows the comparison between both techniques, together with their corresponding references. The path given was a sinusoidal reference in the heave axis, here it is important to remark that we are interested in the spatial result (we follow a path not a trajectory). From this figure it is possible to see how the SMRC technique completes the path 13.5 seconds faster, which represents a 15% improvement.

Fig. 9, shows the signals of the SMRC measured over the robot. We could remark that between time 0 s and 20 s there is no saturation, so that the SMRC loop is inactive and the system goes at the speed fixed by  $\lambda_d$ . During the time 20 s to 35 s the robot goes into a closer part of the path where the speed imposed for  $\lambda_d$  can not be followed, as a

result saturation occurs in actuators. Then, the auxiliary loop switches  $w$  to slow the reference, in such a way that the positional error is reduced. This can be seen in figure 7 where a "bum" in the SMRC reference is noticed.

In this last condition the SMRC loop makes the path reference to advance at the maximum speed which respect the saturation limits (see fig. 10). After this condition is over the SMRC loop is inactive again until the time 58 s where this condition is repeated. Some additional remarks to emphasize are that:

- The step time in the robot was 0.1 seconds. From the simulations conducted using smaller step times, the results tend to be better and the control signals more softy.
- The classical controller utilized was a PD due to the nature of the system, that includes integral action.

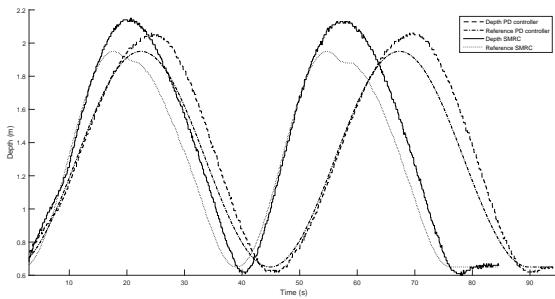


Fig. 7. Path comparison between PD controller and SMRC

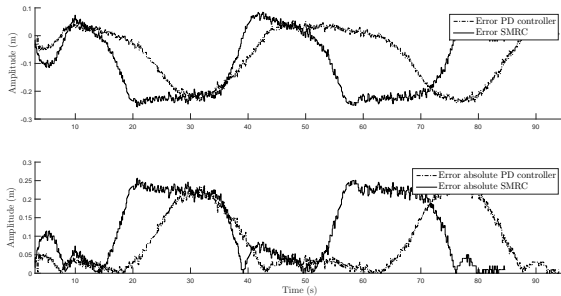


Fig. 8. Error comparison between PD controller and SMRC

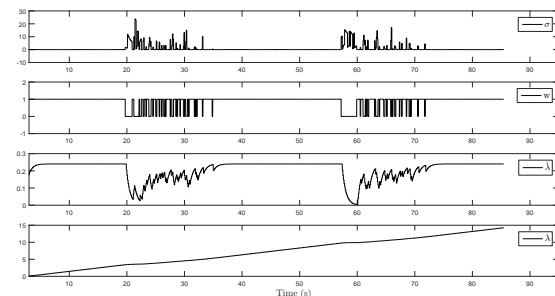


Fig. 9. SMRC signals

## 5. CONCLUSION

In this work a dynamical model (and its corresponding simulator) that could be generalized to any AUVs cuboid

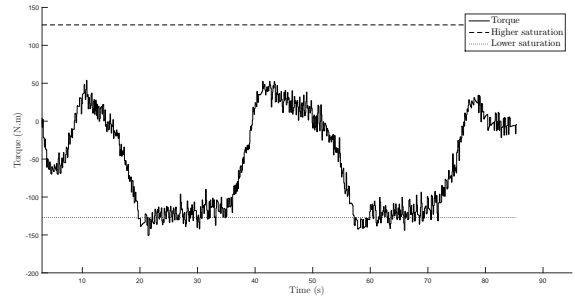


Fig. 10. Torque with SMRC

shape has been proposed and validated through a real test over Ciscrea robot. From this we obtain a useful tool and an efficient methodology. It is expected to future implementations of the simulator, that knowing several parameters of an AUV prototype arrive to model the expected behavior, in order to anticipate possible control problems.

Regarding the SMRC technique applied to the dynamic control of the AUV, which is the novelty of this work, it is possible to conclude that the technique works well and reduces the path tracking time. However, the tuning of the parameters must be done more carefully than in cinematic control framework. Another issue that arises is the way to compensate the slow dynamic of the system. Limitation over internal variables using the same scheme are partial solutions to explore in the future.

## REFERENCES

- Fossen, T.I. (2002). *Marine control systems: Guidance, navigation and control of ships, rigs and underwater vehicles*. Marine Cybernetics Trondheim.
- Garelli, F., Gracia, L., Sala, A., and Albertos, P. (2010). Switching algorithm for fast robotic tracking under joint speed constraints. *Control & Automation (MED), 2010 18th Mediterranean Conference on Control & Automation*.
- Garelli, F., Mantz, R.J., and Battista, H.D. (2011). *Advanced Control for Constrained Processes and Systems*. IET Control engineering series 75. The Institution of Engineering and Technology, London, United Kingdom.
- Nechev, D. and Uchiyama, M. (1997). Singularity-consistent path planing and motion control throught instantaneous self-motion singularities of parallel-link manipulators. *Journal of Robotic Systems*, 14, no. 1, 27–36.
- Nenchev, D. (1995). Tracking manipulator trajectories with ordinary singularities: a null space-based approach. *International Journal of Robotics Research*, 14, no.4, 399–404.
- SNAME (1950). Nomenclature for treating the motion of a submerged body through a fluid. *Technical and Reserach Bulletin*, pp. 115.
- Utkin, V., Guldner, J., and Shi, J. (2009). *Sliding Mode Control in Electro-Mechanical Systems, 2nd ed.* Automation and Control Engineering Series. Taylor Francis.
- Yang, R., Clement, B., Mansour, A., Li, M., and Wu, N. (2015). Modeling of a complex-shaped underwater vehicle for robust control scheme. *J Intell Robot Syst*.